

Effects of Wind Load on the Mechanics of a PV Power Plant

^{1,*}Pascal Romer, ¹Kishan Bharatbhai Pethani, ¹Andreas J. Beinert

¹ Fraunhofer Institute for Solar Energy Systems ISE,
Freiburg, Germany, Heidenhofstraße 2, 79110 Freiburg i.Br., Germany

*Corresponding author, e-mail to: pascal.romer@ise.fraunhofer.de

ABSTRACT: In contrast to the IEC 61215, in real life applications PV modules must withstand inhomogeneous load distributions, for example caused by wind. This work investigates the wind effects onto a PV power plant, containing ten rows with 40 modules each, using computational fluid dynamics simulations coupled to a mechanical finite element method model. The paper focuses on the impact of three factors on the mechanical stability of a PV power plant, namely: Module orientation, wind direction and module inclination angle. A crosswind scenario is found to be most critical. Furthermore, higher module inclination angles result in higher stresses. Finally, general thermomechanical rules are extracted allowing for a deeper understanding of the underlying effects, and therefore help to build more robust PV module installations in the future.

Keywords: FEM; CFD; Wind; Simulation; PV Module; Mechanics

1 INTRODUCTION

For photovoltaic (PV) modules it is mandatory to withstand a homogeneous mechanical load of at least 2400 Pa to pass certification according to IEC 61215-2:2021 [1]. However real-life application shows more often inhomogeneous load distributions on modules instead of homogeneous ones, e.g. due to wind loads. Such inhomogeneous loads can lead to significantly different states of stress compared to the homogeneous ones leading to fatal damage such as cell or glass breakage in the worst case [2].

There are many papers available that determine the wind load on modules using computational fluid dynamics (CFD) simulations or experiments [3–8]. However, none of these papers calculated the occurring stress states of wind loads passed onto a mechanical finite element method (FEM) simulation. In order to close the existing knowledge gap this paper simulates the wind load on a representative section of a PV power plant and determines the resulting stresses of the highest loaded PV module. Finally, the influence of module orientation, wind direction as well as module inclination angle is analyzed.

This is an abridged version of a paper currently in the review process [9].

2 METHODS

2.1 CFD simulations

In the CFD simulations, a representative section of a PV power plant, consisting of 10 rows of PV modules and the mounting rack is simulated. Each row consists of 40 modules with a 20×2 (portrait) or a 10×4 (landscape) arrangement. The influence of the wind direction and the module inclination angle is then examined using the portrait orientation. The simulated parameters are shown in Table I, where bold values correspond to the reference model.

Table I: Varied parameters within the CFD simulation, where bold values are taken for the reference.

Parameter	Values
Module orientation	Landscape, portrait
Module inclination angle [°]	0, 15, 30, 35 , 40, 45, 60, 70
Wind direction [°]	0 , 15, 30, 45, ..., 180

The boundary conditions used in the CFD simulation are shown color-coded in Figure 1. Rigid walls with a vanishing wind speed are the floor (light orange) and the PV modules with the mounting rack (brown). The sidewalls (light blue) as well as the top surface (not shown) are simulated as open boundaries with vanishing stress. An outlet boundary condition with vanishing pressure was assumed for the back side (dark blue). Ultimately, an inlet with a specified wind speed from DIN EN 1991-1-4 [10] type 2, was assumed on the front side (green). The corresponding wind direction is indicated by the wind rose.

To obtain this wind profile, the base wind speed v_{Base} is processed according to:

$$v_{Wind}(z) = 1.3 v_{Base} \quad ; z \leq 4 \text{ m}$$

$$v_{Wind}(z) = 1.45 v_{Base} \left(\frac{z}{10}\right)^{0.12} \quad ; z \geq 4 \text{ m}$$

Based on the CFD simulations, the PV module with the highest wind pressure is identified and both the average and the maximum wind pressure on the front and rear are evaluated. The difference between the rear and the front pressure is referred to as the resulting pressure in the following.

Table II: Material properties of the reference PV module. *: provided by manufacturer, †: measured.

Layer	Material	Density [g/cm ³]	Young's modulus [GPa]	Poisson's ratio [-]	CTE [10 ⁻⁶ K ⁻¹]
Front glass	Soda-lime glass	2.5*	70*	0.2*	9*
Encapsulant	EVA	0.96 [15]	T-dep.†	0.4 [15]	T-dep.†
Solar cell	Cz-Silicon	2.329 [15]	Elasticity matrix [15]	0.29 [15]	T-dep. [13,14]
Backsheet	TPT	2.52 [15]			
Frame	Aluminium	2.7 [16]	70 [16]	0.33 [16]	23 [16]
Frame-inlay	Rubber	0.067*	0.0074*	0.3*	769*

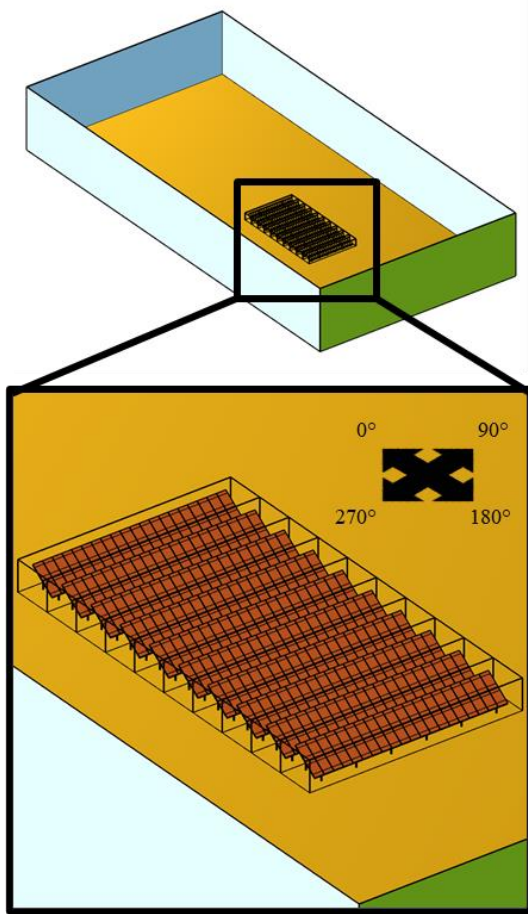


Figure 1: Geometry used in the CFD simulations of the reference portrait configuration. Orange and brown boundaries are simulated as solid walls, light blue boundaries as open boundaries, dark blue boundaries as outlets and the green boundary as an inlet. The wind rose depicts the wind direction.

2.2 Mechanical simulations

The mechanical FEM model consists of a 120 half-cell PV module with the overall size of 1773.1 x 1072.1 mm² and is based on previous works with neglected metallization and ribbons [11,12]. In contrast to the model mentioned, a complete PV module must be simulated in this work due to the inhomogeneous load distribution. Additionally, geometric nonlinearity is considered in this paper. Furthermore, the PV modules production process, consisting of soldering and lamination, is neglected in this work in order to study the pure wind load induced stress. The used material properties are summarized in Table II.

The wind loads calculated in the CFD simulation are

set in the mechanical FEM simulation as surface loads on the front glass and the backsheet.

Due to the brittleness of glass and silicon, the evaluation of the mechanical FEM simulation focuses on the first principal stress in these two layers.

3 RESULTS AND DISCUSSION

With pure head wind, as it is simulated in the reference model, the first row of PV modules blocks the wind from the ones behind, depicted in Figure 3. Therefore, the modules with the highest resulting wind pressure are in the first row. Note that a negative resulting pressure corresponds to a load facing towards the rear of the module and vice versa.

3.1 Module orientation

In a first step a portrait orientation is compared to a landscape orientation. The wind pressure on the front of the module is shown in Figure 2. If this is offset against the wind pressure on the backside (not shown), the resulting maximum pressure is -780 Pa for the portrait orientation and -760 Pa for the landscape orientation. The resulting mean pressure is found to be -610 Pa for the portrait orientation and -640 Pa for the landscape orientation.

The implementation of those pressures in the mechanical FEM simulation leads to a marginal stress difference of 0.6 MPa in the solar cells and 0.3 MPa in the glass, shown in Figure 2 (middle and bottom).

To sum up:

1. Modules in landscape orientation face a marginally higher amplitude in the first principal stress (below 1 MPa) compared to those in portrait orientation.

3.2 Wind direction

For a fixed module inclination angle of 35°, the wind direction α_{wind} is varied between 0° (headwind) and 180° (tailwind) in increments of 15°. Both the average and the maximum resulting pressure (not shown due to the same trend than the average pressure) show a maximum amplitude in the suction pressure of -840 Pa and -1840 Pa respectively, at a wind direction of 45°. At a wind direction of 135° and 120°, the average and the maximum resulting pressure show a maximum in the amplitude of 950 Pa and 1920 Pa, respectively.

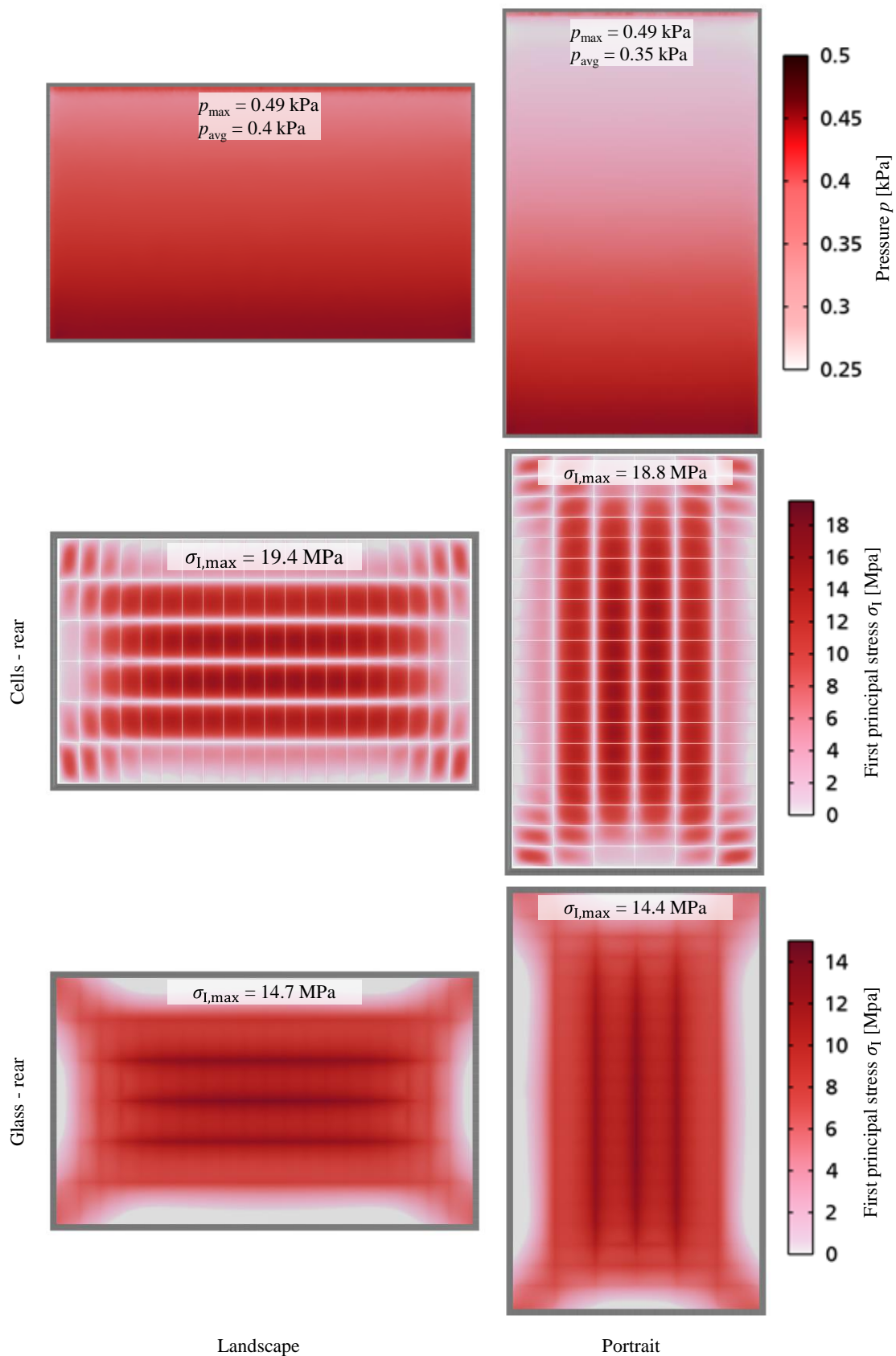


Figure 2: Front side pressure simulated by CFD (top) alongside the first principal stress in the cells (middle) and the frontglass (bottom) both simulated by mechanical FEM for a landscape(left) and portrait (right) orientation.

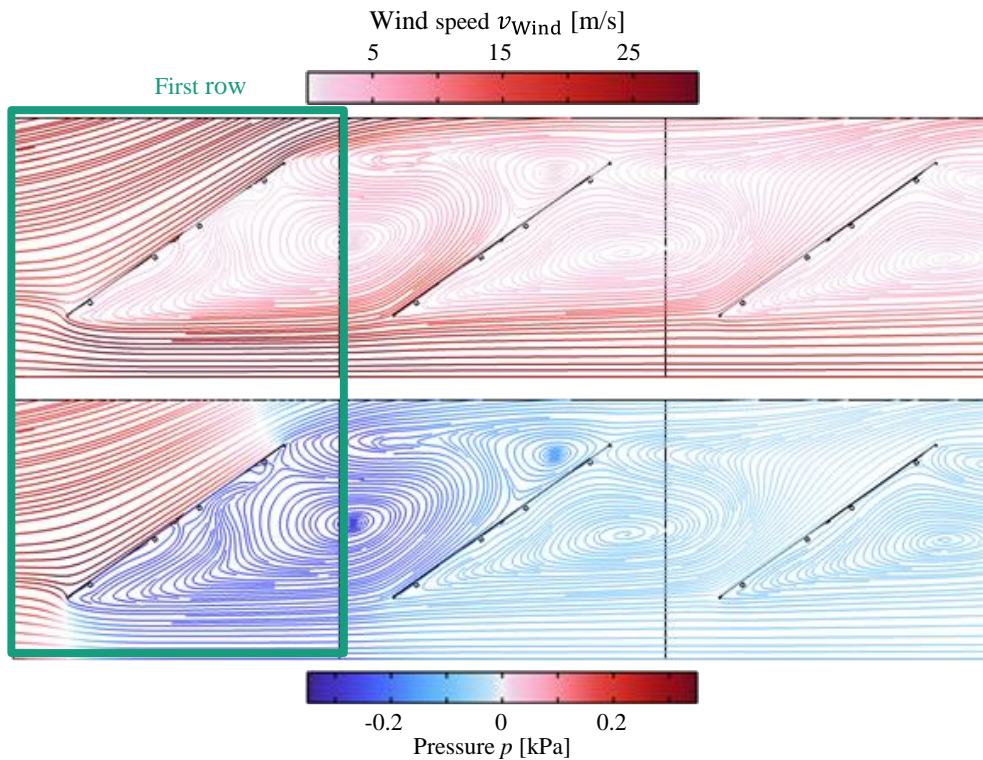


Figure 3: Cut plane through the center modules of the first three rows of PV modules with the wind speed at the top and the pressure at the bottom. In the back rows, the resulting pressure is significantly lower than in the front rows.

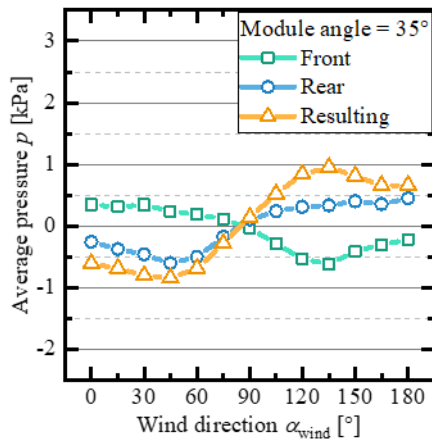


Figure 4: Average pressure on modules front (green) and rear side (blue) and the resulting pressure (orange) at wind directions between 0° and 180° with a module inclination angle of 35°.

Figure 5 shows the resulting first principal stress and the z-displacement for the different wind direction. Note that here and in the following, a negative z-displacement corresponds to a deformation in the direction of the modules rear site. As with the wind pressure, the z-displacement and the first principal stress also show peaks at 45° and 135°. Due to the position of the solar cells below the neutral axis within the PV module, the stress peak at 45°, corresponding to a downward deformation, is more pronounced with 23.2 MPa than the one at 135° with 14.7 MPa. Consequently, for the glass, with its top surface above the neutral axis, the peak at 135° is more

pronounced with 22.1 MPa compared to the one at 45° with 17.9 MPa.

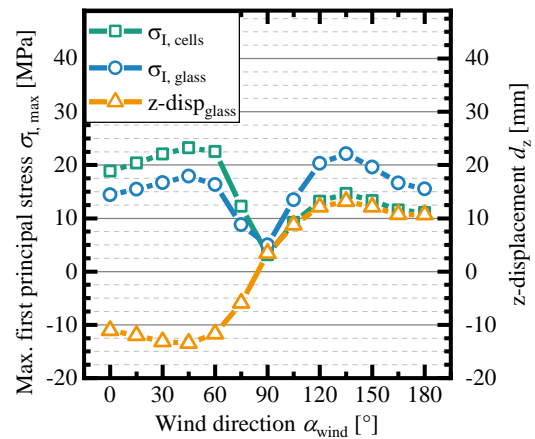


Figure 5: First principal stress in solar cells (green) and glass (dark blue) alongside the PV modules z-displacement (orange) for wind directions between 0° and 180°.

To sum up:

2. Cross wind (45° and 135°) is more critical than head (0°), tail (180°) and side (90°) wind.
3. In a glass-foil module, head wind scenarios are more critical for the solar cells, whereas tail wind scenarios are more critical for the front glass, due to the position relative to the neutral axis.

3.3 Module inclination angle

The module inclination angle β_{module} is varied between 0° and 75° for a wind direction of 45° , being the wind direction with the highest wind pressure. The average and the maximum resulting pressure are shown in Figure 6 and Figure 7, respectively. While the average resulting pressure increases monotonically with the module inclination angle up to -950 Pa at 75° , a peak with -1800 Pa occurs at a module inclination angle of 35° in the maximum resulting pressure. This peak is caused by vortices arising on the modules rear side.

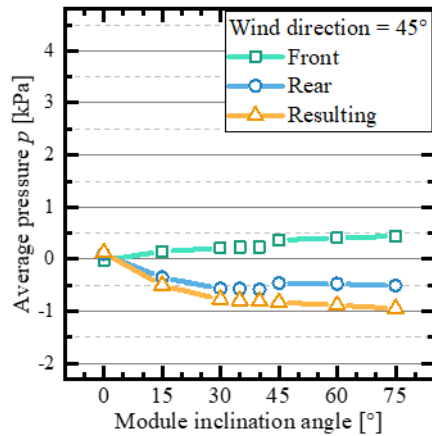


Figure 6: Average pressure on modules front (green) and rear side (blue) and the resulting pressure (orange) at module inclination angles between 0° and 75° with a wind direction of 45° .

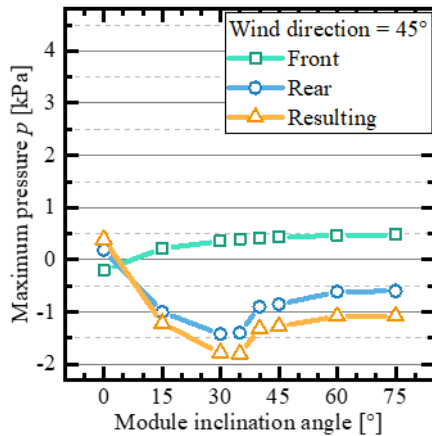


Figure 7: Maximum pressure on modules front (green) and rear side (blue) and the resulting pressure (orange) at module inclination angles between 0° and 75° with a wind direction of 45° .

The z-displacement and the maximum first principal stress in both solar cells and glass can be seen in Figure 8. The mechanical FEM simulation shows an increase of the z-displacements amplitude towards higher inclination angles. While the first principal stress in the cells and the glass, also follows the general trend of the average resulting pressure, additionally a local peak occurs at a module inclination angle of 35° . This is exactly the angle at which the maximum resulting pressure peak occurs.

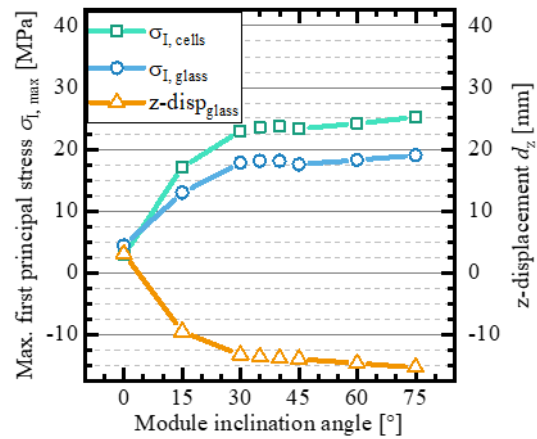


Figure 8: First principal stress in solar cells (green) and glass (dark blue) alongside the PV modules z-displacement (orange) for a module inclination angle between 0° and 75° with a wind direction of 45° .

To sum up:

4. Higher module inclination angles lead to a higher first principal stress.
5. The global trend in the first principal stress and the z-displacement is determined by the resulting average pressure.
6. Peaks in the resulting maximum pressure can cause local maxima in the first principal stress.

4 CONCLUSIONS

The influence of wind on the mechanics of solar modules is systematically examined. The influencing variables module orientation, wind direction and module inclination angle are considered. With a difference of less than 1 MPa, the influence of the module orientation is negligible. In contrast, the other two parameters, wind direction and module inclination angle, have a significant impact on the resulting first principal stress. The highest first principal stresses occur with 23.2 MPa in solar cells with a wind direction of 45° and 22.1 MPa in the front glass at a 135° direction of wind. However, it is worth to note, that all simulated stresses are not critical and correspond to a low probability of fracture. Looking at the module inclination angle, the first principal stress increases globally with increasing angle. However, a local peak develops at a module inclination angle of 35° . This is caused by turbulence at the rear of the module at this angle.

These general rules, regarding the influence of wind on the mechanics of PV modules, are derived:

1. Cross wind (45° and 135°) is more critical than head (0°), tail (180°) and side (90°) wind.
2. In a glass-foil module, head wind scenarios are more critical for the solar cells where tail wind scenarios are more critical for the front glass, due to the position relative to the neutral axis.
3. Higher module inclination angles lead to a higher first principal stress.
4. The global trend in the first principal stress and the z-displacement is determined by the resulting average pressure.
5. Peaks in the resulting maximum pressure can cause local maxima in the first principal stress.

REFERENCES

- [1] International Electrotechnical Commission (IEC), IEC 61215-2:2021 Terrestrial photovoltaic (PV) modules – Design qualification and type approval: Part 2: Test Procedures 2, accessed 21 April 2021.
- [2] P. Romer, A.J. Beinert, Effects of inhomogeneous snow load on the mechanics of a PV module, in: Proceedings of the 38th European Photovoltaic Solar Energy Conference and Exhibition (EU PVSEC), 2021, pp. 602–606.
- [3] M. Shademan, R.M. Barron, R. Balachandar, H. Hangan, Numerical simulation of wind loading on ground-mounted solar panels at different flow configurations, *Can. J. Civ. Eng.* 41 (2014) 728–738. <https://doi.org/10.1139/cjce-2013-0537>.
- [4] S.-T. Hsu, H.-H. Hsieh, Non-Uniform Mechanical Loads due to Wind Effect on Photovoltaic Module, in: Proceedings of the 33rd European Photovoltaic Solar Energy Conference and Exhibition (EU PVSEC), 2017, pp. 1698–1701.
- [5] S.-T. Hsu, T.-C. Wu, Simulated Wind Action on Photovoltaic Module by Non-uniform Dynamic Mechanical Load and Mean Extended Wind Load, *Enrgy Proced* 130 (2017) 94–101.
- [6] S.-T. Hsu, Standardization Work of Non-Uniform Wind Loads Test on PV Module, 37th European Photovoltaic Solar Energy Conference and Exhibition (2020) 894–899. <https://doi.org/10.4229/EUPVSEC20202020-4CO.3.2>.
- [7] C.M. Jubayer, H. Hangan, Numerical simulation of wind effects on a stand-alone ground mounted photovoltaic (PV) system, *Journal of Wind Engineering and Industrial Aerodynamics* 134 (2014) 56–64. <https://doi.org/10.1016/j.jweia.2014.08.008>.
- [8] C.M. Jubayer, H. Hangan, A numerical approach to the investigation of wind loading on an array of ground mounted solar photovoltaic (PV) panels, *Journal of Wind Engineering and Industrial Aerodynamics* 153 (2016) 60–70. <https://doi.org/10.1016/j.jweia.2016.03.009>.
- [9] Pascal Romer, Kishan Bharatbhai Pethani, Andreas J. Beinert, Effect of Inhomogeneous Loads on the Mechanics of PV Modules, *Progress in Photovoltaics: Research and Applications* in review.
- [10] Deutsches Institut für Normung e.V. (DIN), Eurocode 1: Einwirkungen auf Tragwerke - Teil 14: Allgemeine Einwirkungen, Windlasten: Eurocode 1: Einwirkungen auf Tragwerke - Teil 1-4: Allgemeine Einwirkungen, Windlasten, Beuth Verlag GmbH, 2005, p. 147.
- [11] A.J. Beinert, P. Romer, M. Heinrich, M. Mittag, J. Aktaa, H. Neuhaus, The Effect of Cell and Module Dimensions on Thermomechanical Stress in PV Modules, *IEEE J. Photovoltaics* 10 (2020) 70–77. <https://doi.org/10.1109/JPHOTOV.2019.2949875>.
- [12] P. Romer, G. Oreski, A.J. Beinert, D.H. Neuhaus, M. Mittag, More Realistic Consideration of Backsheets Coefficient of Thermal Expansion on Thermomechanics of PV Modules, in: Proceedings of the 37th European Photovoltaic Solar Energy Conference and Exhibition (EU PVSEC), 2020, pp. 772–776.
- [13] R.B. Roberts, Thermal expansion reference data: silicon 300-850 K, *Journal of Physics D: Applied Physics* 14 (1981) L163-163.
- [14] R.B. Roberts, Thermal expansion reference data: silicon 80-280K, *Journal of Physics D: Applied Physics* 15 (1982) L119-120.
- [15] U. Eitner, S. Kajari-Schroeder, M. Koentges, H. Altenbach, Thermal stress and strain of solar cells in photovoltaic modules, in: H. Altenbach, V.A. Eremeyev (Eds.), *Shell-like Structures: Non-classical Theories and Applications*, Springer, Berlin/Heidelberg, 2011.
- [16] W.M. Haynes (Ed.), *CRC handbook of chemistry and physics*, CRC Press, 2014.